Theoretical Study of C_2H_2 Adsorbed on Low-Index Cu Surfaces

W. Liu, J. S. Lian, and Q. Jiang*

Key Laboratory of Automobile Materials, Ministry of Education, and Department of Materials Science and Engineering, Jilin University, Changchun 130022, China

Received: June 17, 2007; In Final Form: September 24, 2007

Ab initio density functional theory was used to determine the adsorption systems of C_2H_2 on Cu (100), (111), and (110) surfaces. Infinitely large models with three-dimensional periodic boundary conditions are implemented in these adsorption systems. The results show that the Cu(100) surface was modified from "square" to "rhombus" through the charge redistribution caused by adsorbing the C_2H_2 molecules. This reveals that the interaction energy dominates the adsorption system rather than the adsorption energy, which involves large deformation. The interaction energy values of C_2H_2/Cu systems on different surfaces have a sequence of C_2H_2/Cu(110) < C_2H_2/Cu(100) < C_2H_2/Cu(111). The tilting angle of the H atom is proportional to chemical binding of the systems.

1. Introduction

Organic molecular adsorption on metallic surfaces is a critical phenomenon in heterogeneous catalysis, tribology, electrochemistry, and material processing.[1] The adsorption system of acetylene (C_2H_2) on Cu surfaces has initiated much scientific interest as it involves notable elementary catalytic reactions, such as the trimerization reaction of C_2H_2 to form benzene on Cu substrates.[2,3] In general, C_2H_2 always decomposes on transition metal surfaces (such as Pd, Pt, Ni, and Rh) at low temperature, and the adsorption behaviors of C_2H_2 on these surfaces are different.[4] In particular, the trimerization reaction of C_2H_2/Cu is unique due to the formation of complex molecules on the metal surfaces.[5] Recent research has demonstrated that Cu is a much more versatile C_2H_2 coupling catalyst than Pd. This is because C_2H_2 trimerization on Cu surface is far less structure sensitive than on the Pd surface, and the adsorbate mobility is also higher.[3] In addition, unlike ethylene (C_2H_4) and ethane (C_2H_6) molecules, the adsorbed C_2H_2 molecule rearranges its geometry and changes its intramolecular binding significantly, which provides insight into the fundamental chemistry of triple C−C bonds on the metallic surfaces.[6,7]

For the C_2H_2/Cu(100) system, Arvanitis et al.[8] found that C_2H_2 molecules lie on substrates as determined by near-edge X-ray absorption fine structure (NEXAFS), but did not give definitive adsorption sites and orientations. Subsequently Hu et al.[9] analyzed the NEXAFS spectra by the multiple-scattering cluster (MSC) method, and detected that C_2H_2 molecules adsorb on the "2-fold aligned bridge" site of Cu(100) surface, shown as type I in Figure 1. However, observation with scanning tunneling microscopy (STM) and inelastic tunneling spectroscopy (IETS) contradicts the aforementioned results.[10,11] It exhibits that the "4-fold diagonal hollow" should be the most preferable site; i.e., C_2H_2 adsorbs on the hollow site of the Cu(100) surface, with the plane of the molecule across the diagonal of the four Cu atoms with square configuration (type V in Figure 1).[2] This has been verified through the determination of charge transfer from Cu to C_2H_2 by Konishi et al.[12]

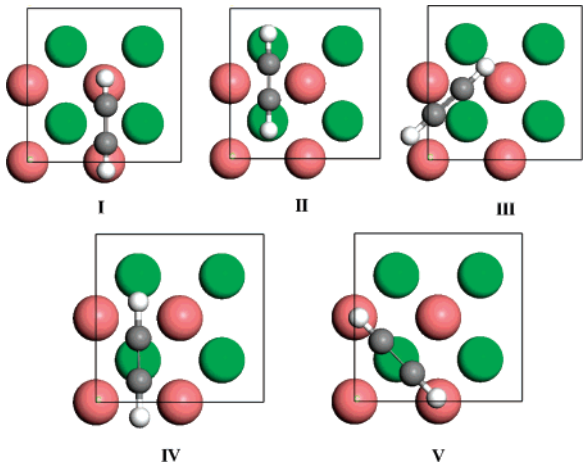

Figure 1. All possible adsorption configurations of the C_2H_2/Cu(100) system: I, "2-fold aligned bridge"; II, "2-fold perpendicular bridge"; III, "3-fold hollow"; IV, "4-fold aligned hollow"; and V, "4-fold diagonal hollow". The largest sphere shows a Cu atom, the middle size sphere is a C atom, and the smallest sphere is a H atom.

For the C_2H_2/Cu(111) system, Bao et al.[13] suggested that the C−C axis is parallel to the Cu(111) surface over a bridge site, but no information about H was given from photoelectron diffraction. Kyriakou et al.[3] reported temperature-programmed reaction of C_2H_2 coupling on the Cu(111) surface, and observed not only benzene formation but also the formation of butadiene and cyclooctatetraene. Except for the C_2H_2/Cu(100) and C_2H_2/Cu(111) systems, the C_2H_2/Cu(110) system has also been investigated by Outka et al.,[14] the results of which indicate that the C_2H_2 adsorption and desorption occurred over a wide temperature range from 280 to 375 K. Avery[15] studied the adsorption and reactivity of the C_2H_2/Cu(110) system using high-resolution electron energy loss (EEL) and thermal desorption spectroscopies. Öström et al.[16] analyzed the chemical bonding and geometric structure of the C_2H_2/Cu(110) system using X-ray photoelectron spectroscopy (XPS), X-ray absorption spectroscopy (XAS), and X-ray emission spectroscopy (XES). However, to the best of our knowledge, no distinct adsorption geometry has been reported for the C_2H_2/Cu(110) system.

* Author to whom correspondence should be addressed: Fax: +86 431 85095876. E-mail: jiangq@jlu.edu.cn.

10.1021/jp0746852 CCC: $37.00 © 2007 American Chemical Society
Published on Web 11/16/2007

From the above analysis, the mechanism behind the C_2H_2/Cu interaction is still not clear. Furthermore, the underlying relationships among geometry, energy, and electronic orbital are rarely investigated due to the complications of characterization for H atoms and also the hybridized orbitals between C−C, C−H, and C−Cu atoms.[17,18] However, since a catalytic reaction is strongly influenced by the molecular conformation and the orbital hybridization, a detailed investigation of the adsorption structures and charge transfer at the single-molecule level is eagerly awaited.[2,12]

Calculations performed with density functional theory (DFT) provide fundamental knowledge of the interaction between adsorbates and metallic surfaces when combined with the complementary results of the experimental data.[19−21] The binding information, which is difficult to measure experimentally, can be used to explain the trends of catalytic behavior and the mechanism of reactant−catalyst interactions.[4] For the C_2H_2/Cu(100) system, Mingo and Makoshi[7] obtained the inelastic scanning tunneling image of the C_2H_2/Cu(100) system using a Green function linear combination of atomic orbitals (LCAO) technique, which is in good agreement with the experimental results. Later, Yuan et al.[22] calculated the binding energies, geometries, and vibrational frequencies of this system using the LCAO method with cluster models. Bernardo and Gomes[6] studied the C_2H_2/Cu(100) system systemically; five possible adsorption sites were proposed with the optimized geometry and energy. Subsequently, a "4-fold aligned hollow" was suggested as the preferable adsorption site. This may be a result of problems involving the cluster modeling of metal surfaces.[6] Olsson et al.[23,24] reported a theoretical and experimental study of chemisorption parameters and STM images for the C_2H_2/Cu(100) system, where the geometric and electronic structure and vibrational energies were obtained from DFT calculations. For the C_2H_2/Cu(111) system, Witko et al.[25] used a cluster model with only four Cu atoms with one located in the first layer and the other three in the second layer. Hermann et al.[26] developed cluster models with more complex geometry variations. However, it is believed that cluster models are not suitable to describe the adsorption systems because they can merely represent finite surfaces. In addition, although these studies described the preferred C_2H_2 binding site for the individual surface, it is difficult to make direct comparisons among the calculations performed on the different surfaces. Therefore, it is essential to systematically study the adsorption behaviors of C_2H_2 on Cu (100), (111), and (110) surfaces, using identical conditions for an infinitely large periodic model.

In our work, larger simulation models with periodic boundary conditions are employed to study the C_2H_2/Cu adsorption systems systematically. The most stable adsorption sites are determined by comparing their corresponding adsorption energy E_{ad} and interaction energy E_{int}. The orientations of C_2H_2 molecules and Cu substrates, the related geometric parameters, and the charge transfer information are also achieved. The simulation results correspond to available experimental and theoretical results in the open literature.

2. Calculations

All DFT calculations are performed in DMol^3 code.[27,28] A uniform generalized gradient approximation with the revised Perdew−Burke−Ernzerhof method is used as the exchange-correlation function.[29] The DFT semicore pseudopotentials (DSPP) core treat method[30] is implemented for relativistic effects, which replaces core electrons by a single effective potential. To ensure that the results of the calculations are directly comparable, identical conditions are employed for all adsorption systems. The *k*-point is set to 5 × 5 × 1 for all slabs, which brings out the convergence tolerance of energy of 2.0 × 10^{-5} hartree (1 hartree = 27.2114 eV), maximum force of 0.004 hartree/Å, and maximum displacement of 0.005 Å.

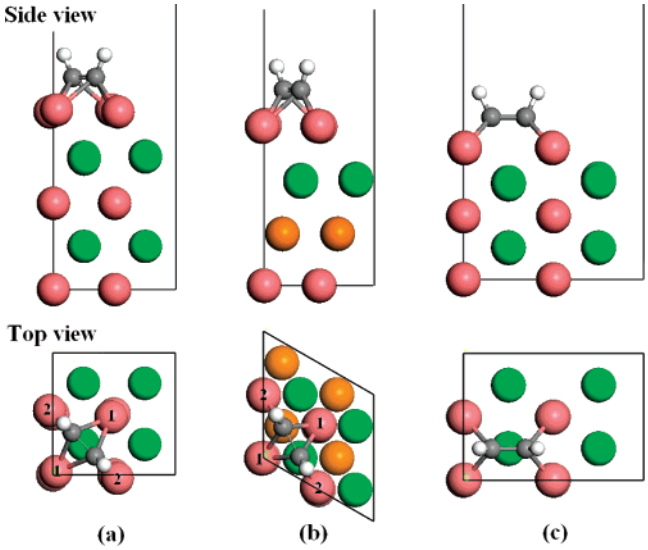

Figure 2. Preferred adsorption structures: (a) C_2H_2/Cu(100), (b) C_2H_2/Cu(111), and (c) C_2H_2/Cu(110). The largest sphere shows a Cu atom, the middle size sphere is a C atom, and the smallest sphere is a H atom.

For free C_2H_2, the initial d_{CC} and d_{CH} values are set to 1.20 Å and 1.06 Å, respectively, which are consistent with those obtained from the experiments.[31] For the Cu(100) surface, a five-layer slab is used to represent the metallic substrate, which makes the topmost and lowermost layers the same, as shown in Figure 2a. Similarly, a four-layer slab and a five-layer slab are used to represent the Cu(111) and Cu(110) surfaces, respectively. All these slabs are separated by a 12 Å vacuum thickness, which ensures that the interaction between the periodically repeated slabs along the normal of the surface is small enough. The above two layers of the slabs are allowed to relax in all energy calculations.

For the individual system, the C_2H_2 molecule is adsorbed on one surface of the Cu slabs, where a uniform (2 × 2) unit cell is set with a C_2H_2 coverage of 0.25 monolayer (ML). There are five possible adsorption configurations, namely "2-fold aligned bridge" (type I), "2-fold perpendicular bridge" (type II), "3-fold hollow" (type III), "4-fold aligned hollow" (type IV), and "4-fold diagonal hollow" (type V).[6,9] Since the surfaces of Cu (110), (100), and (111) have physical and chemical properties similar to those of 2-fold, 4-fold and 6-fold symmetry, respectively, only the possible geometries of the C_2H_2/Cu(100) system are shown in Figures 1 and 2.

E_{ad} describes the bond strength between the gas-phase molecule C_2H_2 and the metallic surfaces, which is calculated by

$$E_{ad} = E_t - (E_{slab} + E_{mole}) \quad (1)$$

where the subscripts "t", "slab", and "mole" denote the total amount of the considered system and the corresponding "clean" slabs and "free" C_2H_2 molecules.[32,33]

Normally C_2H_2/Cu adsorption is accompanied by a large deformation of H tilting and an intensive elongation of the C−C bond. Therefore, the E_{int} value is also given for each adsorption case, which represents the bonding strength between C_2H_2 and

TABLE 1: Comparison of Our Calculated Adsorption Energy E_{ad} and Interaction Energy E_{int} Values (in eV/molecule) for All Possible Adsorption Configurations[a]

	C_2H_2/Cu(100)					C_2H_2/Cu(111)				
	I	II	III	IV	V	I	II	III	IV	V
$-E_{ad}$	0.48	(1.38)[b]	(1.38)	1.22	1.38	0.45	(1.17)	(1.17)	(1.17)	1.17
$-E_{int}$	2.32	(4.08)	(4.08)	3.88	4.08	2.69	(3.95)	(3.95)	(3.95)	3.95
	C_2H_2/Cu(110)-long[c]					C_2H_2/Cu(110)-short[c]				
	I	II	III	IV	V	I	II	III	IV	V
$-E_{ad}$	(1.13)	0.56	0.99	1.13	(1.13)	0.55	0.81	0.99	0.67	(1.13)
$-E_{int}$	(4.17)	1.71	3.97	4.17	(4.17)	2.11	3.79	3.97	3.60	(4.17)

[a] The meanings of types I−V are the same as those in Figure 1. [b] The parentheses indicate that the configurations are unstable, and convert to the most stable ones spontaneously after full relaxation. Thus, their E_{ad} values are the same as those of the most stable ones. [c] C_2H_2 may adsorb along the [001] and [110] directions of Cu(110), since the unit cell of the (110) surface is a rectangle.

TABLE 2: Computed Interaction Energies E_{int} (in eV/molecule) and Geometric Parameters (Bond Angle of C−C−H α in deg and Bond Length *d* in Å) for the Most Stable Adsorption Structures[a]

	bond type	$-E_{int}$	α	d_{CC}	d_{CH}	d_{CCu_1}	d_{CCu_2}	α′	d_{CC}′	d_{CH}′
								120[23]	1.36[23]	1.09[23]
(100)	double	4.08	119.55	1.37	1.08	2.23	1.96	117.6[22]	1.38[22]	1.11[22]
								150[9 b]	1.30[9 b]	
(111)	double	3.95	121.05	1.37	1.08	2.11	2.05	120[26]	1.36[26]	
								130[17]	1.48 ± 0.10[13]	
(110)	single	4.17	115.77	1.38	1.09	2.06	2.06			
free C_2H_2	triple		180	1.20	1.06			180[6]	1.22[6]	1.07[6]
								180[31]	1.20[31]	1.06[31]

[a] α′ and *d*′ are cited theoretical[6,22,23,26] and available experimental results.[9,13,17,31] The C−C bond types are also listed. [b] The values are measured based on the incorrect "2-fold aligned bridge" adsorption site.[9]

the substrate with the deformed geometry. In the computer simulations[32,34]

$$E_{int} = E_t - (E_{slab}' + E_{mole}') \quad (2)$$

where E_{slab}' and E_{mole}' are the energies of Cu substrate and the deformed C_2H_2 molecule, respectively, in the fully relaxed adsorption system. With this definition, the negative E_{ad} and E_{int} values correlate to a stable adsorption.

3. Results and Discussion

The calculated E_{ad} and E_{int} values are listed in Table 1. For the C_2H_2/Cu(100) system, if type V is used as a reference, the E_{ad} values of types I and IV are 0.90 and 0.16 eV/molecule larger, respectively. It is of interest to note that type V was converted from initial configurations of types II and III spontaneously once the full relaxation took place. Therefore, type V is the most stable adsorption site for C_2H_2/Cu(100), which agrees with the experimental observations.[2,10,11] However, if the cluster models with 12 Cu atoms in the first layer and 5 Cu atoms in the second layer are employed, the calculated E_{ad} values have the order II > I > III > V > IV, which differs from the experimental results.[6] For the C_2H_2/Cu(111) system, $E_{ad,I} = -0.45$ eV/molecule is 61.54% greater than $E_{ad,V} = -1.17$ eV/molecule, while the other three types convert to type V after the full relaxation. Therefore, type V is also the most preferable site for the C_2H_2/Cu(111) system, which corresponds to the experimental observations from the EEL[15] and NEXAFS,[17] as well as STM and IETS.[12] Different from the (100) and (111) surfaces, the unit cell of the Cu(110) surface is a rectangle. Thus, C_2H_2 may lie along the [001] (long) or [110] (short) direction of the Cu(110) surface, as shown in Figure 2c. Comparing with the data of E_{ad} listed in Table 1, type IV is the preferred adsorption site in the C_2H_2/Cu(110) system. Since Cu(110) is the most active surface among the three surfaces,[35] the geometry of C_2H_2 adsorption should be very interesting.

Since E_{int} considers both E_{ad} and deformation energy E_{def}, it should be more accurate than only considering the E_{ad} in the adsorption systems that involve severe deformation. In Table 1, $E_{int} \ll E_{ad}$ for the individual type; thus the deformation is crucial for C_2H_2/Cu due to $E_{int} = E_{ad} + E_{def}$. In terms of the E_{int} values, type V is also the preferred adsorption site for C_2H_2/Cu(100) and C_2H_2/Cu(111) systems, and type IV is the one for C_2H_2/Cu(110) system. In addition, if the three most stable adsorption systems are considered, $E_{int(100)} = -4.08$ eV/molecule, $E_{int(111)} = -3.95$ eV/molecule, and $E_{int(110)} = -4.17$ eV/molecule. The E_{int} value decreases with the following sequence: (111) > (100) > (110); the sequence of the adsorption ability is (110) > (100) > (111). This result is in good agreement with the order of γ values of Cu surfaces.[35]

Table 2 shows the detailed geometric parameters for the most stable adsorption structures. For the free C_2H_2 molecule, the determined $d_{CC} = 1.20$ and $d_{CH} = 1.07$ Å are exactly the same as those obtained from the experiments.[31] In the relaxed C_2H_2/Cu(100) system, $d_{CC} = 1.36$ Å, $d_{CH} = 1.08$ Å, and $\alpha = 119.55°$, which agree with the available theoretical results.[22,23] Note that $d_{CC} = 1.36$ Å is 13.33% longer than that of the free molecule, giving direct and reliable information for the degree of hybridization to the substrate.[8,25] Our finding in $\alpha = 119.55°$ is different from the reported $\alpha' = 150°$ that was calculated with the cluster models.[9] For the C_2H_2/Cu(111) system, our calculated $d_{CC} = 1.37$ Å, $d_{CH} = 1.08$ Å, and $\alpha = 121.05°$ correspond to both theoretical[26] and experimental results.[13,17] In addition, our new finding for the C_2H_2/Cu(110) system is $d_{CC} = 1.38$ Å, $d_{CH} = 1.09$ Å, $d_{CCu} = 2.06$ Å, and $\alpha = 115.77°$. It suggested that the distortion leads to C_2H_2 orbitals coupling with the substrate more effectively than those of the free linear molecule.[25] Therefore, the adsorbate distortion is essential for these adsorption systems. From the α values in Table 2, it is discernible that the H atom tilts severely from the Cu(110) surface, implying that H obtains more charges from (110) than from (100) or (111) surfaces.

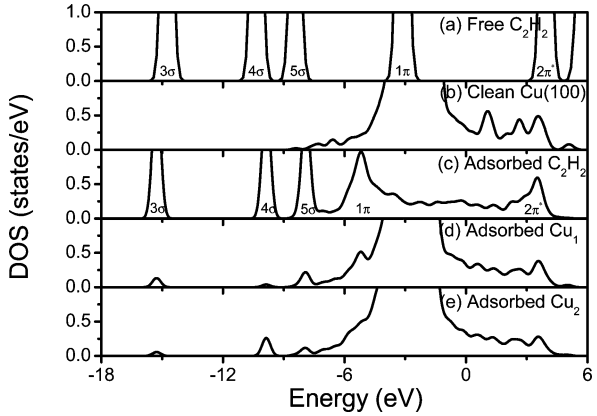

Figure 3. DOS plots for the C_2H_2/Cu(100) system: (a) free C_2H_2 molecule, (b) clean Cu(100) surface, (c) adsorbed C_2H_2 molecule, (d) adsorbed Cu_1, and (e) adsorbed Cu_2. The Fermi level is located at 0 eV.

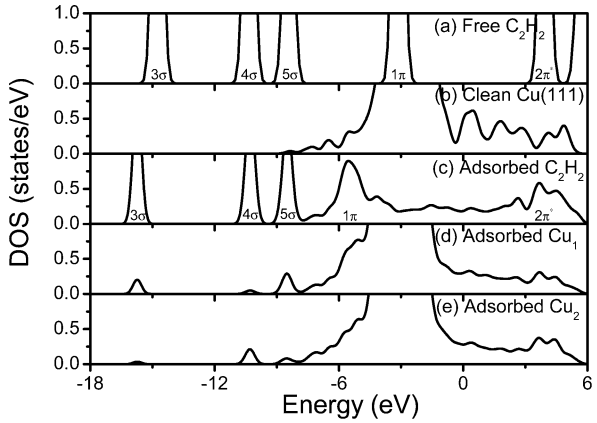

Figure 4. DOS plots for the C_2H_2/Cu(111) system: (a) free C_2H_2 molecule, (b) clean Cu(111) surface, (c) adsorbed C_2H_2 molecule, (d) adsorbed Cu_1 atom, and (e) adsorbed Cu_2 atom. The Fermi level is located at 0 eV.

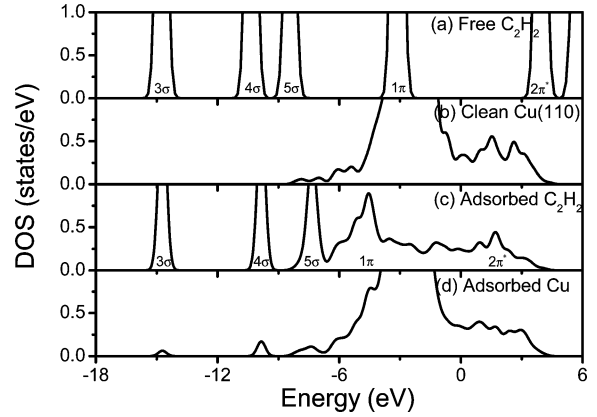

Figure 5. DOS plots for the C_2H_2/Cu(110) system: (a) free C_2H_2 molecule, (b) clean Cu(110) surface, (c) adsorbed C_2H_2 molecule, and (d) adsorbed Cu. The Fermi level is located at 0 eV.

The C−C bond types are also listed in Table 2. The most profound phenomenon is that the free C−C triple bond converts to a single bond due to the adsorption on Cu(110) surfaces. This phenomenon is different from what occurs on the (100) and (111) surfaces that have only one broken bond. This indicates that C_2H_2 is substantially rehybridized when adsorption occurs on Cu(110) (C−C bond length is sp^3-like) compared with C_2H_2/Cu(100) and C_2H_2/Cu(111). Therefore, C_2H_2/Cu(110) has the strongest chemical binding. From the above analysis, the variations of d and α are proportional to the chemical binding

TABLE 3: Hirshfeld Charge Values of C and H Before and After Adsorption[a]

	states	C	H	ΔC_2H_2
(100)	after	−0.1792	+0.0255	0.1537
	before	−0.0923	+0.0923	
(111)	after	−0.1764	+0.0303	0.1461
	before	−0.0923	+0.0923	
(110)	after	−0.1835	+0.0163	0.1672
	before	−0.0923	+0.0923	

[a] ΔC_2H_2 indicates the charge difference of C_2H_2 induced by adsorption.

of C_2H_2/Cu; i.e., the lower E_{int} value results in the longer C−C bonds and the larger degree of H tilts. Therefore, the binding strength trend between adsorbate and substrate can be roughly estimated by the corresponding geometries.

As shown in Figure 2a, the four topmost Cu atoms are no longer in the same positions after adsorption. Cu_1 and Cu_2 denote the lateral and frontal Cu atoms with respect to the C−C chain. It is discernible that the two Cu_1 atoms are "compressed" with the Cu_1-Cu_1 atomic distance shortening from 3.62 to 3.25 Å, while two Cu_2 atoms are "elongated" with the Cu_2-Cu_2 distance expanding from 3.62 to 4.00 Å. These lead to variations in the configuration of the four Cu atoms from "square" to "rhombus". Note that the differences of Cu_1 and Cu_2 have not been noticed in any previous work, although the distortions of C_2H_2 were widely observed. From Table 2, $d_{CCu_1} = 2.23$ Å is 13.78% longer than $d_{CCu_2} = 1.96$ Å in the C_2H_2/Cu(100) system. In the C_2H_2/Cu(111) system, $d_{CCu_1} = 2.11$ Å is 2.93% longer than $d_{CCu_2} = 2.05$ Å as listed in Table 2. Two Cu_1 atoms are also "elongated" with the Cu_1-Cu_1 atomic distance expanding from 2.56 to 2.69 Å, while two Cu_2 atoms are "compressed" from 4.43 to 4.29 Å. In the following context, the differences of Cu_1 and Cu_2 will be further clarified in the aspect of electronic structures. In addition, the vertical distances between C and the first Cu layer are 1.24, 1.35, and 1.42 Å for (110), (100), and (111) surfaces, respectively, which also correlates to the E_{int} trends.

In the aspect of the bonding mechanism, it is widely accepted that the Dewar−Chatt−Duncanson (DCD) model gives a good picture for unsaturated hydrocarbons on metal surfaces.[36,37] In terms of this model, the C_2H_2 1π orbital donates charge into empty Cu orbitals, while the occupied metal d orbital back-donates charge into an empty C_2H_2 2π* orbital, simultaneously. This charge transfer leads to a loss of bond order and increased C−C bond distance, which is consistent with our results. Subsequently, a "spin-uncoupling" model was proposed, which states that E_{int} is a balance of the rehybridization cost and the energy gain from the formation of bonds near the surface.[38,39] For the C_2H_2/Cu system, this process is made by that C atoms are first excited from the sp (triple C−C bond) to the sp^2 (double C−C bond) state, and prepared for bonding with the substrates. Obviously, this energy cost, which is an essential part of E_{int}, can be seen as the driving force to deform the molecule, because deformation occurs with C−C bond type changes.[38] Then, the bonding to the surface is formed through the loss of π* electron charge and gain in the π states, which is the same as the prediction of the DCD model. Note that the spin-uncoupling model has indeed some advantages; for example, the energy cost values and the barriers between physisorbed and chemisorbed states can be estimated in certain cases.[40]

Furthermore, the density of states (DOS) of C_2H_2 on Cu was determined to investigate the variations of orbital hybridizations. Figure 3 shows the DOS plots of the C_2H_2/Cu(100) system. The free C_2H_2 molecule and the clean Cu(100) surface are also

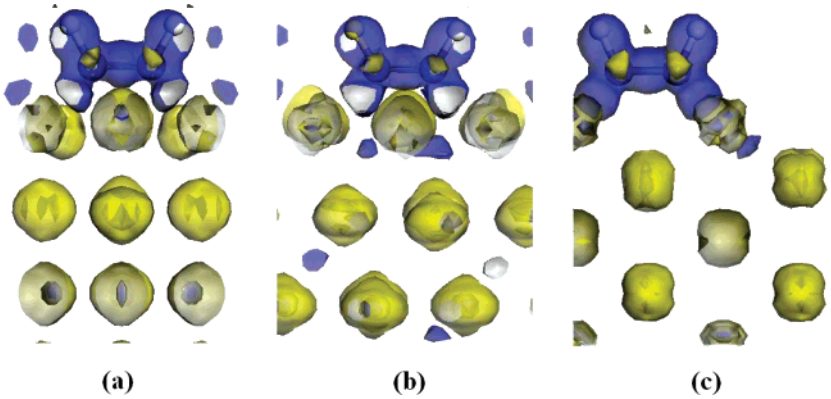

Figure 6. Plots of the electron density difference: (a) C_2H_2/Cu(100), (b) C_2H_2/Cu(111), and (c) C_2H_2/Cu(110). The blue region shows the electron accumulation, while the yellow region shows the electron loss.

depicted in the figure. For the free C_2H_2 molecule (see Figure 3a), compared with the molecular orbitals proposed by Jorgensen et al.[41] and the photoemission peaks from the experiments,[42] it was found that the four peaks located at −14.75, −10.35, −8.45, and −3.13 eV are 3σ (or $2\sigma_g$), 4σ (or $2\sigma_u$), 5σ (or $3\sigma_g$), and 1π (or $1\pi_u$) orbitals, respectively, where 1π is the highest occupied molecular orbital (HOMO). The band range above the Fermi level is defined as the $2\pi^*$ (or $1\pi_g$) orbital, which is the lowest unoccupied molecular orbital.[42] Comparing Figure 3a with Figure 3b, no peak overlaps between the free C_2H_2 and the clean Cu(100) surface. After adsorption, the C sp orbitals undergo a rehybridization to form Cu−C bonds. Therefore, the C_2H_2 molecule has to be restructured by increasing its C−C distance and also bending its CH ends.[26] As shown in Figure 3c, the 5σ and 1π orbitals were broadened, thus dominating the interaction. It can been seen that the 1π obital shifts significantly from −3.13 to −5.20 eV, while the 5σ moves slightly to the Fermi level.[42] For Cu, the orbitals of Cu_1 move left to hybridize with the adsorption of the C_2H_2 molecule (see Figure 3d). A sharp new peak composed by the Cu_1 4s and Cu_1 3d orbitals appears at −5.20 eV and interacts with the C_2H_2 1π orbital (HOMO). Since the HOMO plays an important role in the reaction, the appearance of this new peak is critical. In the lower energy range, the new peak located at −7.94 eV reveals the interaction in the C_2H_2 5σ orbital. For the Cu_2 atoms, no peak hybridizes with the HOMO of the C_2H_2 molecule, and the intensity is much weaker than that of Cu_1 when Cu_2 interacts with the C_2H_2 5σ orbital. However, the new peak located at −9.90 eV is detected, demonstrating the interaction between the Cu_1 and the lower C_2H_2 4σ orbital as shown in Figure 3e. This evidences the difference of Cu_1 and Cu_2 based on the DOS plots. The Cu_1 tightly connects with the adsorbed molecule. This notion is also supported by the data from Hirshfeld charge analysis.[43] From our calculations, the Hirshfeld charge of Cu_1 and Cu_2 increases from −0.0069 to +0.1006 and +0.0561, respectively, indicating that Cu_1 donates nearly twice the amount of charges to C_2H_2 as Cu_2.

The DOS plots of the C_2H_2/Cu(111) system and the clean Cu(111) surface are shown in Figure 4. Comparing Figure 4a with Figure 4b, two new Cu_1 peaks located at −5.10 and −8.53 eV exhibited a strong interaction in the orbitals of C_2H_2 1π and C_2H_2 5σ, respectively. Different from the C_2H_2/Cu(100) system, both new peaks can also be detected for Cu_2 atoms with relative low intensities (Figure 4c). The Hirshfeld charges of Cu_1 and Cu_2 increase from −0.0059 to +0.0849 and +0.0683. From the above analysis, the differences between the Cu_1 and Cu_2 atoms in Cu(111) are smaller than those in Cu(100), although the charge movement from Cu_1 to C_2H_2 is much more in Cu(100).

Figure 5 shows the DOS plots for the C_2H_2/Cu(110) system. Differing from the (100) and (111) surfaces, the shapes of all four Cu atoms remain the same after adsorption. In this figure, Cu 3s and 4p orbitals interact with the C_2H_2 1π orbital at −4.55 eV. In the lower energy range, each C_2H_2 orbital hybridizes with a Cu peak. From the DOS plots, both adsorbate and substrate states are moved left, implying that the free energies are lowered as adsorption.[44]

The calculated Hirshfeld charge values for both C and H before and after adsorption are listed in Table 3. For the (110) surface, C and H drop from −0.0923 and +0.0923 to −0.1792 and +0.0255 after adsorption, thus resulting in the charge differences (ΔC_2H_2) of 0.1537. Similarly, $\Delta C_2H_2 = 0.1461$ for the (111) surface, and $\Delta C_2H_2 = 0.1672$ for the (110) surface. Thus, ΔC_2H_2 values have the sequence of (110) > (100) > (111). This is induced by the fact that the Cu(110) surface with its higher adsorption ability has the greatest amount of charge transfer, while Cu(111) is the opposite. This verifies our E_{int} order.

The above charge transfer can also be visualized in the plot of electron density variation. As shown in Figure 6, the blue areas show where the electron density has been enriched while the yellow areas show where the density has been depleted. Obviously, the C_2H_2 molecules gain while Cu substrates lose electrons. A similar result of charge transfer has been reported for the saturated hydrocarbons on Cu surface.[45] In Figure 6a, the orbitals of C_2H_2, which lie on the Cu(100) substrate, lead to a larger E_{int} value. From Figure 6b, it is discernible that the orbital hybridization between C_2H_2 and Cu are much weaker than that of Figure 6a, showing a weaker binding strength of C_2H_2/Cu(111). The orbital hybridization between the adsorbate and the Cu(110) surface is the largest among the three surfaces: as shown in Figure 6c, the blue and yellow area are strongly mixed. Some small yellow areas also appear around the C atoms. This is because the charges donated from Cu are not fully accumulated around the C atoms, but partially further transfer to H (even make the H tilt).[25,26] Therefore, the Hirshfeld charge values of H atoms decrease after adsorption.

4. Conclusions

In conclusion, DFT calculations with the DSPP core treatment method are employed to study the adsorption geometry, adsorption energy, and electronic structure of C_2H_2/Cu systems. The "4-fold diagonal hollow" is determined to be the most stable adsorption site for the C_2H_2/Cu(100) and C_2H_2/Cu(111) systems, while the "4-fold aligned hollow" is the most stable site for the C_2H_2/Cu(110) system. Although the highly distorted C_2H_2 molecules are widely studied, the differences between the Cu_1

and Cu_2 atoms are newly revealed. The variation of the electron density was caused by the electrons moving from Cu to C_2H_2. This results in the intermolecular charge redistribution between the C and H.

Acknowledgment. The authors acknowledge financial support from the National Key Basic Research and Development Program of China (Grant 2004CB619301) and the "985 Project" of Jilin University.

References and Notes

(1) Ma, Z.; Zaera, F. *Surf. Sci. Rep.* **2006**, *61*, 229.
(2) Stipe, B. C.; Rezaei, M. A.; Ho, W. *Science* **1998**, *280*, 1732.
(3) Kyriakou, G.; Kim, J.; Tikhov, M. S.; Macleod, N.; Lambert, R. M. *J. Phys. Chem. B* **2005**, *109*, 10952.
(4) Medlin, J. W.; Allendorf, M. D. *J. Phys. Chem. B* **2003**, *107*, 217.
(5) Dvorak, J.; Hrbek, J. *J. Phys. Chem. B* **1998**, *102*, 9443.
(6) Bernardo, C. G. P. M.; Gomes, J. A. N. F. *J. Mol. Struct.* **2003**, *629*, 251.
(7) Mingo, N.; Makoshi, K. *Phys. Rev. Lett.* **2000**, *84*, 3694.
(8) Arvanitis, D.; Wenzel, L.; Baberschke, K. *Phys. Rev. Lett.* **1987**, *59*, 2435.
(9) Hu, X. F.; Chen, C. J.; Tang, J. C. *Surf. Sci.* **1996**, *365*, 319.
(10) Stipe, B. C.; Razaei, M. A.; Ho, W. *Phys. Rev. Lett.* **1999**, *82*, 1724.
(11) Stipe, B. C.; Razaei, M. A.; Ho, W. *Phys. Rev. Lett.* **1998**, *81*, 1263.
(12) Konishi, Y.; Sainoo, Y.; Kanazawa, K.; Yoshida, S.; Taninaka, A.; Takeuchi, O.; Shigekawa, H. *Phys. Rev. B* **2005**, *71*, 193410.
(13) Bao, S.; Schindler, K.-M.; Hofmann, P.; Fritzsche, V.; Bradshaw, A. M.; Woodruff, D. P. *Surf. Sci.* **1994**, *291*, 295.
(14) Outka, D. A.; Friend, C. M.; Jorgensen, S.; Madix, R. J. *J. Am. Chem. Soc.* **1983**, *105*, 3468.
(15) Avery, N. R. *J. Am. Chem. Soc.* **1985**, *107*, 6712.
(16) Öström, H.; Nordlund, D.; Ogasawara, H.; Weiss, K.; Triguero, L.; Pettersson, L. G. M.; Nilsson, A. *Surf. Sci.* **2004**, *565*, 206.
(17) Fuhrmann, D.; Wacker, D.; Weiss, K.; Hermann, K.; Witko, M.; Wöll, Ch. *J. Chem. Phys.* **1998**, *108*, 2651.
(18) Gaudioso, J.; Lee, H. J.; Ho, W. *J. Am. Chem. Soc.* **1999**, *121*, 8479.
(19) Liu, W.; Zhu, Y. F.; Lian, J. S.; Jiang, Q. *J. Phys. Chem. C* **2007**, *111*, 1005.
(20) Liu, L. M.; McAllister, B.; Ye, H. Q.; Hu, P. *J. Am. Chem. Soc.* **2006**, *128*, 4017.
(21) Soon, A.; Todorova, M.; Delley, B.; Stampfl, C. *Phys. Rev. B* **2006**, *73*, 165424.
(22) Yuan, L. F.; Yang, J.; Li, Q.; Zhu, Q. S. *J. Chem. Phys.* **2002**, *116*, 3104.
(23) Olsson, F. E.; Persson, M.; Lorente, N.; Lauhon, L. J.; Ho, W. *J. Phys. Chem. B* **2002**, *106*, 8161.
(24) Olsson, F. E.; Persson, M.; Lorente, N.; Lauhon, L. J.; Ho, W. *J. Phys. Chem. B* **2002**, *106*, 11073.
(25) Witko, M.; Hermann, K. *Appl. Catal., A* **1998**, *172*, 85.
(26) Hermann, K.; Witko, M. *Surf. Sci.* **1995**, *337*, 205.
(27) Delley, B. *J. Chem. Phys.* **1990**, *92*, 508.
(28) Delley, B. *J. Chem. Phys.* **2000**, *113*, 7756.
(29) Hammer, B.; Hansen, L. B.; Nørskov, J. K. *Phys. Rev. B* **1999**, *59*, 7413.
(30) Delley, B. *Phys. Rev. B* **2002**, *66*, 155125.
(31) *Tables of Interatomic Distances and Configuration in Molecules and Ions*; The Chemical Society, Burlington House: London, 1965.
(32) Bocquet, M.-L.; Sautet, P.; Cerda, J.; Carlisle, C. I.; Webb, M. J.; King, D. A. *J. Am. Chem. Soc.* **2003**, *125*, 3119.
(33) Morin, C.; Simon, D.; Sautet, P. *J. Phys. Chem. B* **2004**, *108*, 5653.
(34) Gao, W.; Zhao, M.; Jiang, Q. *J. Phys. Chem. C* **2007**, *111*, 4042.
(35) Jiang, Q.; Lu, H. M.; Zhao, M. *J. Phys.: Condens. Matter* **2004**, *16*, 521.
(36) Dewar, M. J. S. *Bull. Soc. Chim. Fr.* **1951**, *18*, C79.
(37) Chatt, J.; Duncanson, L. A. *J. Chem. Soc.* **1953**, 2939.
(38) Triguero, L.; Pettersson, L. G. M.; Minaev, B.; Ågren, H. *J. Chem. Phys.* **1998**, *108*, 1193.
(39) Triguero, L.; Föhlisch, A.; Väterlein, P.; Hasselström, J.; Weinelt, M.; Pettersson, L. G. M.; Luo, Y.; Ågren, H.; Nilsson, A. *J. Am. Chem. Soc.* **2000**, *122*, 12310.
(40) Nilsson, A.; Pettersson, L. G. M. *Surf. Sci. Rep.* **2004**, *55*, 49.
(41) Jorgensen, W. L.; Salem, L. *The Organic Chemist's Book of Orbitals*; Academic: New York, 1973.
(42) Weinelt, M.; Huber, W.; Zebisch, P.; Steinrück, H.-P.; Ulbricht, P.; Birkenheuer, U.; Boettger, J. C.; Rösch, N. *J. Chem. Phys.* **1995**, *102*, 9709.
(43) Hirshfeld, F. L. *Theor. Chim. Acta B* **1977**, *44*, 129.
(44) Sun, C. Q. *Prog. Solid State Chem.* **2007**, *35*, 1.
(45) Wöll, Ch.; Weiss, K.; Bagus, P. S. *Chem. Phys. Lett.* **2000**, *332*, 553.